

## Release of Toxic Gd<sup>3+</sup> Ions to Tumour Cells by Vitamin B<sub>12</sub> Bioconjugates

Patrizia Siega,<sup>[a]</sup> Jochen Wuerges,<sup>[a]</sup> Francesca Arena,<sup>[b]</sup> Eliana Gianolio,<sup>[b]</sup>  
Sergey N. Fedosov,<sup>[c]</sup> Renata Dreos,<sup>[a]</sup> Silvano Geremia,<sup>\*[a]</sup> Silvio Aime,<sup>\*[b]</sup> and  
Lucio Randaccio<sup>[a]</sup>

*Dedicated to the Centenary of the Italian Chemical Society*

**Abstract:** Two probes consisting of vitamin B<sub>12</sub> (CNCbl) conjugated to Gd chelates by esterification of the ribose 5'-OH moiety, Gd-DTPA-CNCbl (**1**; DTPA = diethylenetriamine-*N,N,N',N'',N'''*-pentaacetic acid) and Gd-TTHA-CNCbl (**2**; TTHA = triethylenetetramine-*N,N,N',N'',N'''*-hexaacetic acid), have been synthesised and characterised. The crystal structure of a dimeric form of **1**, obtained by crystallisation with an excess of GdCl<sub>3</sub>, has been determined. The kinetics of binding to and dissociation from transcobalamin II show that **1** and **2** maintain high-affinity binding to the vita-

min B<sub>12</sub> transport protein. Complex **2** is very stable with respect to Gd<sup>3+</sup> release owing to the saturated co-ordination of the Gd<sup>3+</sup> ion by four amino and five carboxylate groups. Hydrolysis of the ester functionality occurs on the time scale of several hours. The lack of saturation and the possible involvement of the ester functionality in co-ordination result in lower stability of **1** towards hydrolysis and in a considera-

ble release of Gd<sup>3+</sup> in vitro. Gd<sup>3+</sup> ions released from **1** are avidly taken up by the K562 tumour cells to an extent corresponding to approximately 10<sup>10</sup> Gd<sup>3+</sup> per cell. The internalisation of toxic Gd<sup>3+</sup> ions causes a marked decrease in cell viability as assessed by Trypan blue and WST-1 tests. On the contrary, the experiments with the more stable **2** did not show any significant cell internalisation of Gd<sup>3+</sup> ions and any influence on cell viability. The results point to new avenues of in situ generation of cytotoxic pathways based on the release of toxic Gd<sup>3+</sup> ions by vitamin B<sub>12</sub> bioconjugates.

**Keywords:** bioinorganic chemistry • cobalamines • drug delivery • drug design • vitamins

### Introduction

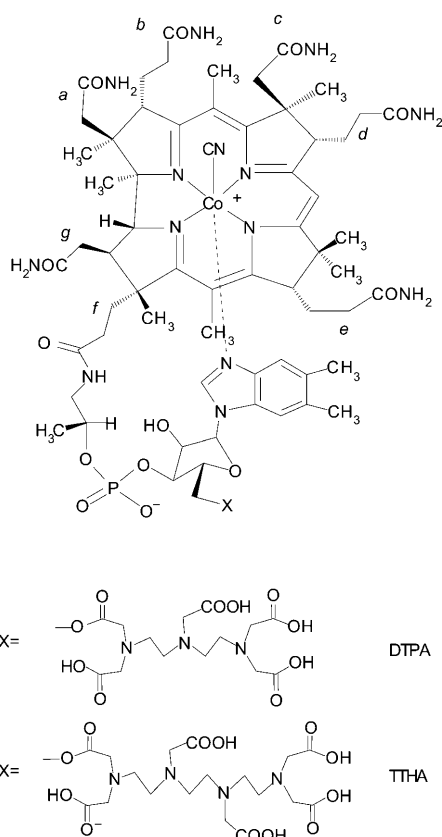
Vitamin B<sub>12</sub>, or more generally cobalamin (Cbl; Scheme 1), is synthesised only by bacteria, but mammalian cells require it as enzyme cofactor in the two forms of methyl-Cbl for methionine synthase and adenosyl-Cbl for methylmalonyl CoA mutase.<sup>[1]</sup> Mammals have developed a specific internalisation pathway for this essential micronutrient, which employs three transport proteins. The vitamin is absorbed through the intestine by intrinsic factor (IF) and transported through the plasma by transcobalamin (TC) and haptocorrin (HC). The TC-Cbl complex is ubiquitously taken up by means of receptor-mediated endocytosis, with subsequent release of Cbl from the protein. Instead, HC was thought to enter only hepatocytes, but was recently found to be taken up by several types of tumour cells as well.<sup>[2]</sup> Events in the intracellular trafficking and conversion of Cbl to the two active forms have still to be revealed in detail.<sup>[3]</sup> Vitamin B<sub>12</sub> is indirectly involved in the synthesis of thymidine monophosphate, and thus DNA, because a catalytically active me-

[a] Dr. P. Siega, Dr. J. Wuerges, Prof. R. Dreos, Prof. S. Geremia, Prof. L. Randaccio  
Department of Chemical Sciences  
Centre of Excellence in Biocrystallography  
University of Trieste, Via Licio Giorgieri 1, 32127 Trieste (Italy)  
Fax: (+39)040-558-3903  
E-mail: sgeremia@units.it

[b] Dr. F. Arena, Dr. E. Gianolio, Prof. S. Aime  
Department of Chemistry, IFM and Center of Molecular Imaging  
University of Turin, Via Nizza 52, 10127 Turin (Italy)  
Fax: (+39)011-670-7855  
E-mail: silvio.aime@unito.it

[c] Dr. S. N. Fedosov  
Protein Chemistry Laboratory, Department of Molecular Biology  
University of Aarhus, Science Park  
Gustav Wieds Vey 10, 8000 Aarhus C (Denmark)

Supporting information for this article is available on the WWW under <http://dx.doi.org/10.1002/chem.200802680>.



Scheme 1. Vitamin B<sub>12</sub> esterified at the 5'-hydroxyl group of the ribose moiety with the X chelate groups, DTPA and TTHA (corrin ring side chains are labelled from a to f according to the standard nomenclature).

thionine synthase also liberates tetrahydrofolate (THF) from the methyl trap upon transfer of a methyl group from methyl-THF to homocysteine by means of Cbl. Consequently, intracellular deficiency in the vitamin leads to impaired cell proliferation in addition to abnormalities of the nervous system and the blood.<sup>[4]</sup> Fast-proliferating cell types require higher amounts of vitamin B<sub>12</sub>. This observation has given considerable potential to the use of vitamin B<sub>12</sub> analogues as imaging agents for diagnosis of these cell types or as therapeutic drugs exploiting the conjugated groups with growth-blocking or cytotoxic properties. Well-characterised examples have been reported.<sup>[5,6]</sup> These include the use of vitamin B<sub>12</sub> analogues 1) to inhibit cell proliferation by modifications on the propionamide side chain e,<sup>[7]</sup> 2) to image tumours with <sup>99m</sup>Tc or <sup>111</sup>In radiolabelled Cbl-*b*-4-aminobutyl-amidediethylenetriaminepentaacetate<sup>[8,9]</sup> or with 3) fluorescently labelled Cbl<sup>[10,11]</sup> and 4) to target the delivery of a cytotoxin (colchicine) to tumours.<sup>[12]</sup> The approach employed in these applications to obtain efficient targeting of imaging or chemotherapeutic drugs is based on up-regulation of the TC-Cbl receptors on the surface of tumour cells in the DNA replication phase<sup>[13,14]</sup> and possibly by higher turnover of the receptors.<sup>[15]</sup> A recent study<sup>[2]</sup> demonstrated that a radiolabelled bioconjugate bound to HC is also able

to target tumour cells, avoiding its undesirable accumulation in organs, which serve as TC-Cbl storage sites, particularly in the kidneys.

Recently, we solved the X-ray crystal structure of TC<sup>[16]</sup> and modelled for homology the structures of the other two B<sub>12</sub> transport proteins, HC and IF.<sup>[17]</sup> The availability of these three-dimensional models permits a rational design of a vitamin B<sub>12</sub> based probe with a high affinity towards the plasma transport proteins that could extend the use of these bioconjugates beyond the radionuclides to paramagnetic ions, such as Gd. Compared with the highly sensitive nuclear and optical imaging techniques, magnetic resonance imaging (MRI) requires much higher amounts of the agent for the visualisation of tumour cells.

Herein we report our studies aimed at exploring the use of Gd-labelled vitamin B<sub>12</sub> probes for targeting tumour cells. Vitamin B<sub>12</sub> appears to be a vector with recognition capabilities that should not be affected by the linkage to the Gd-chelate as happens with peptide-targeting moieties.<sup>[18]</sup> Moreover, it was deemed of interest to endow the probes with the property of disassembling into non-toxic components after a relatively short time. To accomplish this task, we employed the pro-drug diethylenetriamine-*N,N,N',N'',N'''*-pentaacetic acid (DTPA, Scheme 1) and the analogous triethylenetetramine-*N,N,N',N'',N''',N''''*-hexaacetic acid (TTHA, Scheme 1) esterified at the 5'-hydroxyl group of the sugar moiety of vitamin B<sub>12</sub>.

The major difference between these two is the presence of an open Gd<sup>3+</sup> co-ordination shell in the case of DTPA, whereas the higher denticity of TTHA fills all the co-ordination sites of the Gd<sup>3+</sup> ion. We surmised that this diversity should result in significant differences in the ability to release Gd<sup>3+</sup> ions when the probe is anchored at the cell surface as well as in the hydrolysis of the ester linkage. Since the free Gd<sup>3+</sup> ion is extremely toxic, it was deemed of interest to exploit the possibility for the DTPA-vitamin B<sub>12</sub> derivative to specifically deliver and release cytotoxic Gd<sup>3+</sup> ions.

Here, we describe the design, synthesis and characterisation of the bioconjugated complexes with Gd<sup>3+</sup>, that is, Gd-DTPA-CNCbl (**1**) and Gd-TTHA-CNCbl (**2**), including the kinetics of binding and dissociation with TC, the rate of hydrolysis of the ester bond by means of relaxivity measurements and the X-ray structure of the dimeric form of **1**. Finally, to verify the Gd<sup>3+</sup> uptake and to test the toxicity of **1** and **2**, we report the investigation on the cellular internalisation of Gd<sup>3+</sup> ions in the K562 cell line and the relative viability tests.

## Results and Discussion

**Design of the vitamin B<sub>12</sub> bioconjugates:** The X-ray structure of the TC-Cbl complex<sup>[6]</sup> showed that the side chains of the corrin ring (Scheme 1) are largely buried in the interface with the protein and thus do not represent ideal positions for the attachment of conjugates. In the protein, the cobalt

ion of the base-on cobalamin is axially co-ordinated by a histidine side chain. This histidine may be displaced by an externally supplied molecule,<sup>[19]</sup> thereby forming a further potential site for the attachment of bioconjugates to Co. However, inspection of the Cbl environment in human TC (Figure 1) shows that the 5'-hydroxyl group on the ribose of the nucleotide moiety of Cbl is the ideal site to accommodate a molecule of the size of Gd-DTPA without disturbing the interactions between TC and Cbl (Figure 1). Some electrostatic repulsion between Gd-DTPA of net charge -1 and its protein environment is expected as a moderately negative potential is calculated for the protein surface in this region.

**Synthesis and characterisation of DTPA-CNCbl, TTHA-CNCbl and their Gd<sup>3+</sup> derivatives:** The syntheses of the bioconjugates DTPA-CNCbl and TTHA-CNCbl (Scheme 1) are very similar, so that the following discussion applies to both derivatives. The preparation exploits the reaction between the ribose 5'-hydroxyl group of CNCbl and the dianhydride of DTPA or TTHA, following, with some modifications, a previously reported procedure for the esterification with succinic anhydride.<sup>[20]</sup> In particular, a much lower excess of dianhydride (4 equiv) was used to avoid the presence of free DTPA or TTHA in the final product. In fact, we found that the free acid is difficult to remove and interferes severely with the subsequent complexation of Gd<sup>3+</sup>. The degree of formation of the bioconjugates during synthesis and the purity and integrity of the final products (i.e., the absence of free CNCbl) have been checked by polyacrylamide gel electrophoresis (PAGE). In fact, although CNCbl has no net charge, the bioconjugates are negatively charged and their coloured spots can be easily identified.

The bioconjugates are sensitive to hydrolysis of the ester bond when left for one day or more at room temperature (20 °C) in solutions with a pH above 6 (for a quantitative assessment see the section "Hydrolysis of **1** and **2**"), whereas both **1** and **2** are stable for weeks at pH 2 and room temperature. Therefore, the characterisation of solutions of DTPA-CNCbl and TTHA-CNCbl in D<sub>2</sub>O by NMR spectroscopy was carried out at pD = 2.2. The comparison between the reported <sup>13</sup>C NMR spectra of CNCbl<sup>[21]</sup> and those of the bioconjugates shows that, besides the presence of new peaks due to the chelate, almost all the peaks due to the CNCbl moiety undergo very small chemical shift changes. Only the peaks arising from the R4 and R5 carbon atoms (Scheme 2) show a significant chemical shift change (about  $\Delta\delta = -3$  and  $+3$  ppm, respectively). These results are in agreement with the presence of a chemical modification of the ribose-5'-hydroxyl group<sup>[22]</sup> and rule out the formation of a derivative esterified at both 2'- and 5'-OH groups, as was previously reported for the reaction with the smaller succinic anhydride.<sup>[20]</sup>

Complexes **1** and **2** were obtained *in situ* by the addition of a slightly less than stoichiometric amount of GdCl<sub>3</sub> to an aqueous solution of lyophilised DTPA-CNCbl and TTHA-CNCbl, respectively.

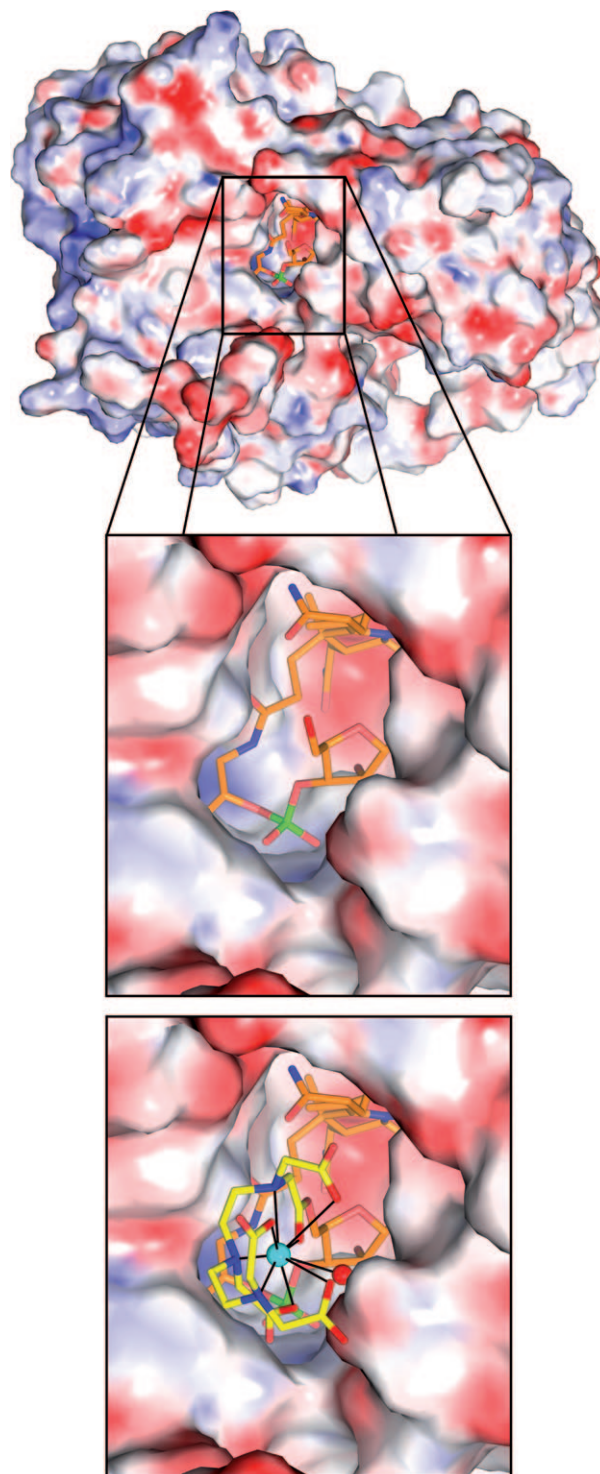
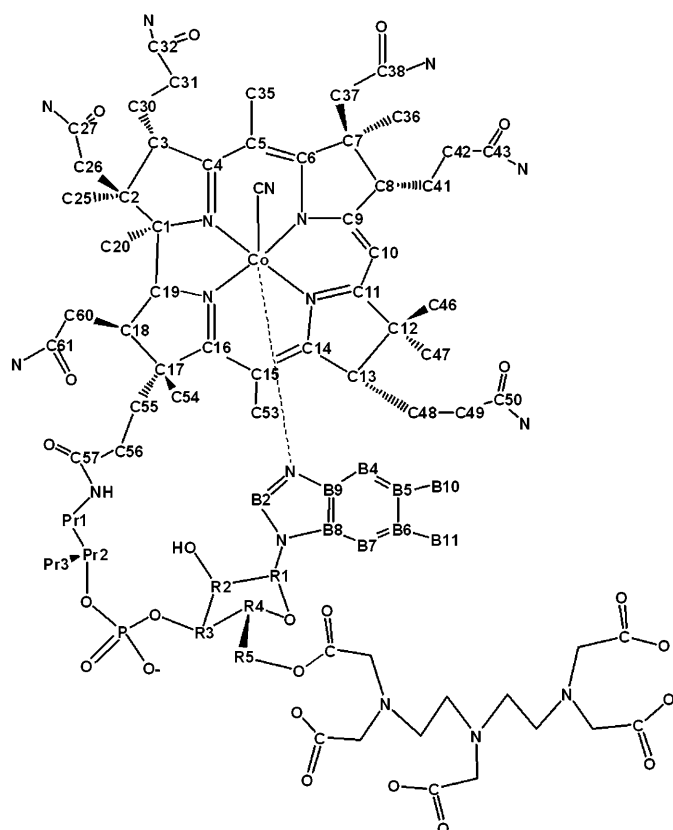


Figure 1. Cbl environment in the human transport protein transcobalamin. The TC structure was previously determined by X-ray diffraction and is presented as a molecular surface coloured according to the electrostatic potential (blue, positive potential; red, negative potential). The close-up of the ligand binding site at the domain interface shows that the 5'-hydroxyl group of the ribose moiety is not covered by amino acids and represents an ideal position for the esterification with one of the carboxylates of the Gd-chelator DTPA. In the close-up at the bottom, DTPA-Gd-H<sub>2</sub>O was attached to the 5'-OH group to model the interactions of the bioconjugate **1** with TC. Colour code: carbon atoms of CNCbl in orange and of DTPA in yellow, oxygen atoms in red, nitrogen atoms in blue, phosphorous in green and gadolinium in cyan.



Scheme 2. <sup>13</sup>C NMR spectra numbering scheme of DTPA-CNCbl.

The attempts to crystallise **1** in the presence of an excess of GdCl<sub>3</sub> led to orthorhombic crystals (space group *C222*<sub>1</sub>) composed of dimeric species (see the Experimental Section). These dimers are formed by two bioconjugate molecules of **1** held together by an additional Gd<sup>3+</sup> ion located on a crystallographic twofold axis (Figure 2). The crystal structure confirms that the attachment of DTPA to CNCbl occurred at the 5'-hydroxyl group of the ribose moiety. The Gd<sup>3+</sup> ion chelated by DTPA is co-ordinated by three nitrogen atoms, four oxygen atoms from four carboxylate groups, one solvent water molecule and one oxygen atom from the phosphate group of a symmetry-related molecule. The last-mentioned co-ordinated oxygen atom, essential for dimer formation in the solid state, is most probably replaced in solution by the oxygen atom of the ester functionality. Also, the additional Gd<sup>3+</sup> ion located in the special position shows a co-ordination sphere of nine ligands. The two symmetry-related molecules co-ordinate this Gd<sup>3+</sup> ion by both oxygen atoms of a carboxylate of DTPA and by another oxygen atom of the phosphate group. The remaining three sites are occupied by water molecules, one of which lies on the same crystallographic twofold axis as the Gd<sup>3+</sup> ion. The ester carbonyl group is involved in an intramolecular hydrogen bond with the propionamide side chain *e*. The CN ligand on the upper axial side of Co is involved in an intermolecular hydrogen bond with the amide nitrogen of the side chain *d*.

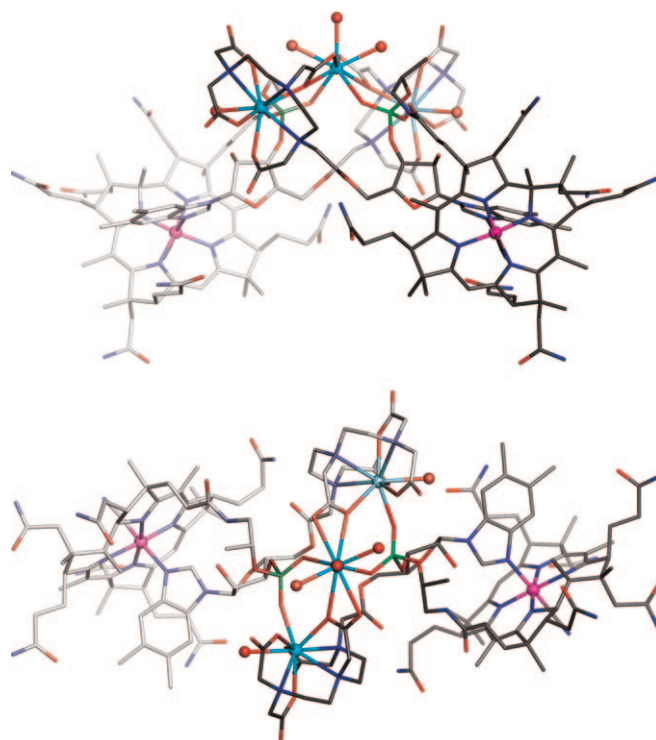


Figure 2. Two views of the crystal structure of the "dimeric form" of **1** determined by X-ray diffraction. The orientation in the top structure is perpendicular to the twofold symmetry axis. In the bottom structure the view is along the twofold symmetry axis, on which one of the Gd<sup>3+</sup> ions (in cyan) and one of the co-ordinated water molecules (in red) are located. Carbon atoms are shown in grey, nitrogen atoms in blue, oxygen atoms in red, cobalt atoms in orange and phosphorous atoms in green.

Three X-ray structures of Cbl acylated at the ribose 5'-OH with small carboxylic acids to protect this site in further functionalisation processes have been recently reported.<sup>[23]</sup>

A survey in the Cambridge Structure Database (CSD) regarding the co-ordination of Gd<sup>3+</sup> shows that the co-ordination number observed in our structure corresponds to the most abundant; about 50% of all deposited structures show 9-coordinate Gd<sup>3+</sup> and half of these include water molecules as ligands. The observed co-ordination distances are in accordance with the average distances calculated from the CSD structures. A particular feature is the coordination environment of the Gd<sup>3+</sup> ion on the twofold symmetry axis. There, the Gd–O distances are significantly longer than those concerning the Gd<sup>3+</sup> chelated by DTPA, a fact that most likely reflects the weaker coordination of the Gd<sup>3+</sup> on the special position. As a consequence, the distance between the chelated and the bridging Gd<sup>3+</sup> (5.0 Å) is at the high end of the range found for the Gd–Gd distance in the CSD analysis (3.7–5.1 Å).

**Hydrolysis of 1 and 2:** The hydrolysis of the ester bond yields CNCbl and Gd–DTPA in **1**, and CNCbl and Gd–TTHA in **2**, respectively. The hydrolysis reactions have been followed by measuring the variation of the proton relaxation rates of the aqueous solutions of **1** and **2** (Figure 3). At

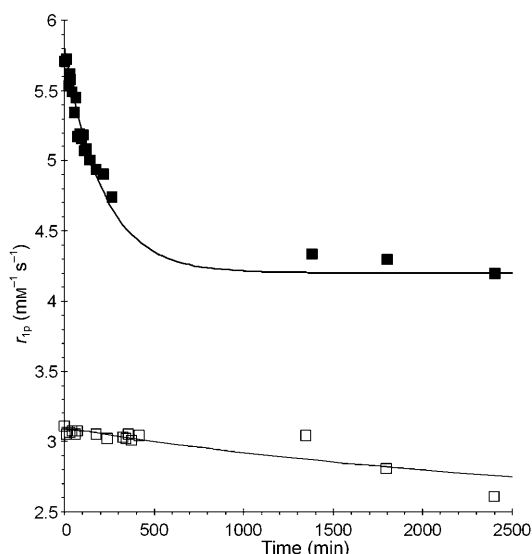


Figure 3. Time courses of the hydrolysis process of complex **1** (■) and **2** (□) in PBS solution at 298 K followed by millimolar relaxivity,  $r_{1p}$ . Lines represent their first-order best fit.

20 MHz and 298 K, complex **1** shows a relaxivity of  $5.7 \text{ mm}^{-1} \text{ s}^{-1}$ , whereas **2** has a relaxivity of  $3.1 \text{ mm}^{-1} \text{ s}^{-1}$ . At the same frequency and temperature conditions, the  $r_{1p}$  values of Gd–DTPA and Gd–TTHA are  $4.2 \text{ mm}^{-1} \text{ s}^{-1}$  and  $2.5 \text{ mm}^{-1} \text{ s}^{-1}$ , respectively.<sup>[24]</sup> In phosphate-buffered saline (PBS, pH 7.2), **1** reaches a value of  $4.7 \text{ mm}^{-1} \text{ s}^{-1}$  after 5 h to indicate a relative rapid hydrolysis of the compound under these conditions. The fitting of experimental data with a first-order equation gave a hydrolysis rate constant of  $(4.7 \pm 3) \times 10^{-3} \text{ min}^{-1}$ .

The hydrolysis rate of **1** was further investigated by both PAGE and  $^{31}\text{P}$  NMR spectroscopy experiments (Figures 1S and 2S in the Supporting Information). In the latter case, to remove the interference of the paramagnetic  $\text{Gd}^{3+}$  ion, the experiments were performed on the Eu analogue of **1** (Eu-**1**). Both techniques confirm that the half-life ( $t_{1/2}$ ) of **1** is 2.5 h.

In contrast, the corresponding transformation of **2** occurs on a much slower timescale. The fitting of experimental data gave a hydrolysis rate constant of  $(3.5 \pm 5) \times 10^{-4} \text{ min}^{-1}$  that corresponds to  $t_{1/2} = 33 \text{ h}$ . The marked difference in the hydrolysis rate of **1** and **2** can be explained by taking into account that DTPA and TTHA moieties are conjugated to the sugar moiety of CNCbl thanks to the transformation of an acetic arm of the chelator into ester functionality. The latter functionality in **1** may still provide an oxygen donor atom to the coordination of the  $\text{Gd}^{3+}$  ion, whereas in the case of **2** the coordination number of 9 of the  $\text{Gd}^{3+}$  ion is saturated by the four nitrogen atoms and five carboxylate groups, thus leaving the sixth carboxylate group in the ester link out of the co-ordination cage.

The relatively fast hydrolysis reaction prevented the determination of the stability constants in terms of  $\text{Gd}^{3+}$  release for **1** and **2**. In fact,  $\text{Gd}^{3+}$  complexes of polyamino–polycarboxylic ligands have generally very high stability

constants with long equilibration times.<sup>[25]</sup> The PAGE experiments proved that **1** and **2** are inert regarding the exchange of bound  $\text{Gd}^{3+}$  at physiological conditions, so that the hydrolysis of the ester bond is faster than the equilibration. It has been reported that the formation of a single ester bond in DTPA decreases the thermodynamic binding constant of  $\text{Gd}^{3+}$  by about  $2 \times 10^3$ ,<sup>[26]</sup> so that the stability constant for **1** may be estimated in between that of Gd–EDTA ( $\log K = 17$ ) and Gd–DTPA ( $\log K = 23$ ). Because the conjugation of CNCbl to TTHA by the ester functionality does not affect the co-ordination of  $\text{Gd}^{3+}$  in **2**, its thermodynamic stability may be considered not too far from that of unconjugated Gd–TTHA ( $\log K = 28$ ).<sup>[25]</sup>

**Binding of 1 and 2 to transcobalamin:** The binding protein TC was interacted with the mixture of **1** or **2** and the fluorescent probe CBC (a fluorescent Cbl analogue)<sup>[27]</sup> taken at different proportions. Formation of the highly fluorescent complex TC–CBC was followed over 0.2 s (Figure 4), and the reaction was simulated with the help of the computer programme Gepasi<sup>[28]</sup> according to a bidirectional irreversible mechanism  $\text{EI} \leftarrow \text{I} + \text{E} + \text{S} \rightarrow \text{ES}$  (E = apoTC, I = CBC, S = **1** or **2**), valid on a short timescale (see refs. [27] and [29] for details). In such an equation, E corresponds to TC, S to Cbl, **1** or **2** and I to CBC. The calculated values of  $k_+$  are shown

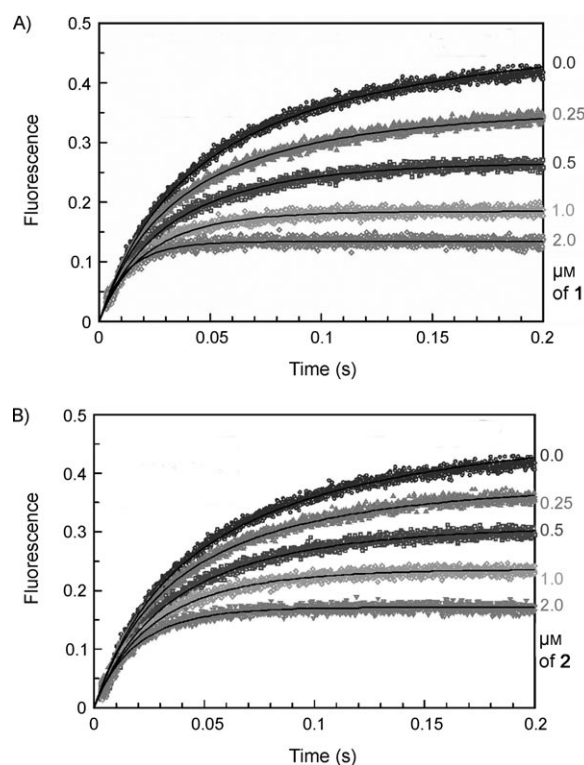


Figure 4. Competitive binding of CBC and A) **1** or B) **2** to the transport protein TC. The protein ( $0.5 \mu\text{M}$ ) was added to the mixture of CBC ( $0.5 \mu\text{M}$ ) and **1** or **2** (0, 0.25, 0.5, 1.0,  $2.0 \mu\text{M}$ ), whereupon the fluorescent response of CBC was followed over time. The amplitude of the fluorescent signal corresponded to  $1.05 \text{ RU} \mu\text{M}^{-1}$ . Calculated binding rate constants are presented in Table 1.

in Table 1. They are similar to those reported earlier for Cbl, CBC and a group of Cbl analogues.<sup>[29]</sup>

Table 1. Binding and dissociation rate constants of cobalamin ligands when interacting with TC (mean ± standard error).

Binding reaction	$k_+ \times 10^{-6}$ [M <sup>-1</sup> s <sup>-1</sup> ]	$k_- \times 10^7$ [s <sup>-1</sup> ]	$K_d$ [M] × 10 <sup>15</sup> = $k_-/k_+$
TC + Cbl ⇌ TC-Cbl <sup>[a]</sup>	68 ± 2	2.5 ± 0.2	3.7 ± 0.3
TC + CBC ⇌ TC-CBC	41 ± 4	4.0 ± 1.0	10.0 ± 2.0
TC + <b>1</b> ⇌ TC- <b>1</b>	34 ± 3	3.4 ± 0.3	10.0 ± 1.0
TC + <b>2</b> ⇌ TC- <b>2</b>	21 ± 3	5.2 ± 0.4	25.0 ± 4.0

[a] Data from ref. [27].

**Dissociation of **1** and **2** from transcobalamin:** Dissociation of **1** and **2** from TC was induced by the external fluorescent probe CBC added in some excess. The dissociation of S from the binding site E-S → E+S is followed by the fast attachment of CBC to the protein E+I → E-I, the first step being rate limiting. The experimental data were fitted by a linear function, because only the initial part of the curve was recorded (Figure 5). The proposed mechanism matches with sufficient accuracy the experimental data throughout

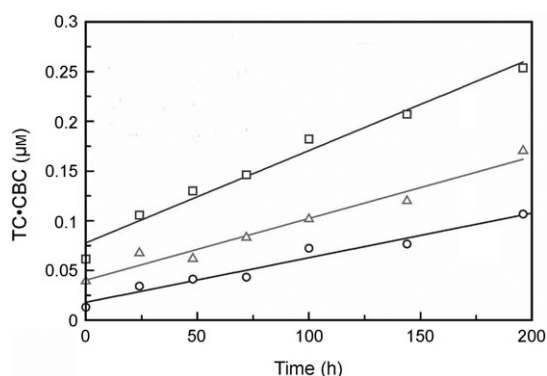


Figure 5. Dissociation kinetics of CNCbl (○), **1** (△) or **2** (□), acting as S, from the transport protein TC. Dissociation was induced by mixing the protein-S complex at 0.5 µM with CBC (1 µM), whereupon substitution of S by CBC was followed as an increase in CBC fluorescence. Calculated dissociation rate constants are presented in Table 1.

the whole diapason of measurements. The linear trends and the slopes of the curves reported in Figure 5 suggest that the hydrolysis rate of the bioconjugates is significantly reduced when they are bound to protein. The “protection” effect of the transport protein towards hydrolysis of **1** and **2** is confirmed by the kinetic experiments performed with the homologue IF protein (see the Supporting Information).

The calculated dissociation rate constants are presented in Table 1. They correspond to the initial slopes ( $v_{-S} = k_{-S} \cdot [ES]$ ) divided by the initial concentration of the protein-ligand complex ES. The ratio  $k_{-S}/k_{+S}$  gives the values of the equilibrium dissociation constants  $K_d$  (see Table 1). The affinity of **1** and **2** for the binding proteins was slightly lower than that of Cbl, but the  $K_d$  values still remain on the level of fM. This seems to be sufficient to guarantee the complete

binding of this Cbl analogue under physiological conditions with TC = 0.5–1 nM.

**Cellular internalisation of Gd<sup>3+</sup> ions from vitamin B<sub>12</sub> targeted probes:** Having established that 50% hydrolysis of **1** and **2** takes place after 2.5 and 33 h, respectively, we went on to assess how much Gd<sup>3+</sup> can be transferred to target cells before the completion of their transformation into the stable Gd-DTPA and Gd-TTHA products. For the internalisation experiment, a myelogenous leukaemia (K562) cell line was considered: approximately 3 to 4 million cells were incubated for 1 h at 37°C under an atmosphere of pCO<sub>2</sub> (5%) in the presence of increasing concentrations of **1** and **2** (Figure 6).

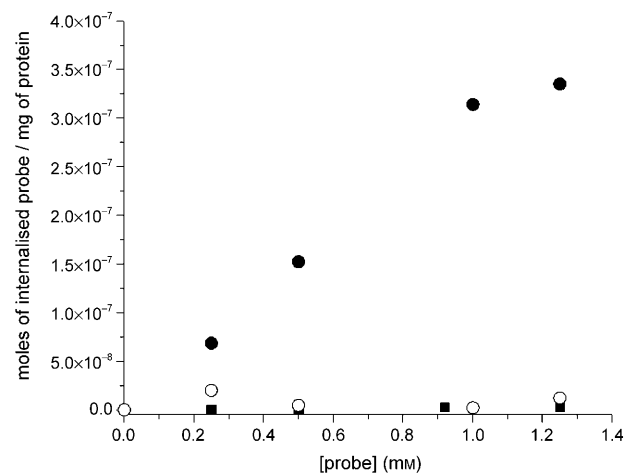


Figure 6. Amount of internalised Gd<sup>3+</sup> in K562 cells as a function of **1** (●) or **2** (■) concentration in the culture medium (37°C, 1 h). Open circles (○) are relative to the amount of internalised CNCbl-containing agent determined by UV absorption at 361 nm.

Whereas **1** showed an increased uptake with the increase of the Gd-containing probe in the medium (with a saturation, corresponding to around 10<sup>10</sup> Gd<sup>3+</sup> per cell, at concentrations higher than 1 mM), **2** led to a negligible internalisation of Gd<sup>3+</sup> at all the investigated concentrations. Although the analytical method used (inductively coupled plasma mass spectrometry, ICP-MS) does not allow one to establish the chemical form of the Gd-containing species, it appears likely that the internalisation process involves free Gd<sup>3+</sup> ions. As it is known that CNCbl has a broad absorption peak centred at 361 nm, this hypothesis has been validated by the parallel measure of the UV absorption at the 361 nm wavelength of the same cell lysates on which Gd<sup>3+</sup> contents have been determined. To determine exactly the concentration of the CNCbl-containing complex in the cell lysates, a calibration curve has been registered by the addition of known amounts of complex **1** to the cell lysates. An extinction coefficient  $\epsilon = 25 \text{ mM}^{-1} \text{ cm}^{-1}$  has been determined that is very close to the value determined in buffer conditions ( $\epsilon = 27 \text{ mM}^{-1} \text{ cm}^{-1}$ ). Because the amount of internalised Gd<sup>3+</sup> has been found to be very high, it was calculated that the probe

concentration in cell lysates should have been high enough to allow the measure of reliable absorbance values. Surprisingly, as shown in Figure 6, in the case of complex **1**, the amount of internalised CNCbl (○) is two orders of magnitude lower than the internalised  $Gd^{3+}$  (●) and comparable to that determined when complex **2** is used (■). This is clear evidence that, in the case of complex **1**,  $Gd^{3+}$  enters the cells as a free ion. Comparison with internalisation tests made by using Gd-DTPA instead of **1** (Figure 7A) allows one to conclude that the CNCbl-targeting moiety is absolutely necessary to obtain high  $Gd^{3+}$  ion uptake by the cells. Further support to this view was brought about by an uptake experiment carried out by incubating K562 cells with increasing concentrations of complex **1** not freshly prepared but rather left in the buffer solution for one day (in Figure 7A 1 mM concentration data is reported). During this time a complete hydrolysis of the ester functionality occurred to give free Gd-DTPA and CNCbl. Under these conditions the amount of internalised  $Gd^{3+}$  is in the range of  $10^{-9}$  moles per mg of proteins. Furthermore, the competition experiment with CNCbl itself corroborates the hypothesis of a direct participation of the vitamin B<sub>12</sub> conjugate for incorporation of  $Gd^{3+}$  into tumour cells. Figure 7B reports the decrease of  $Gd^{3+}$  uptake in K562 cells as a consequence of the addition of increasing amounts of CNCbl to the incuba-

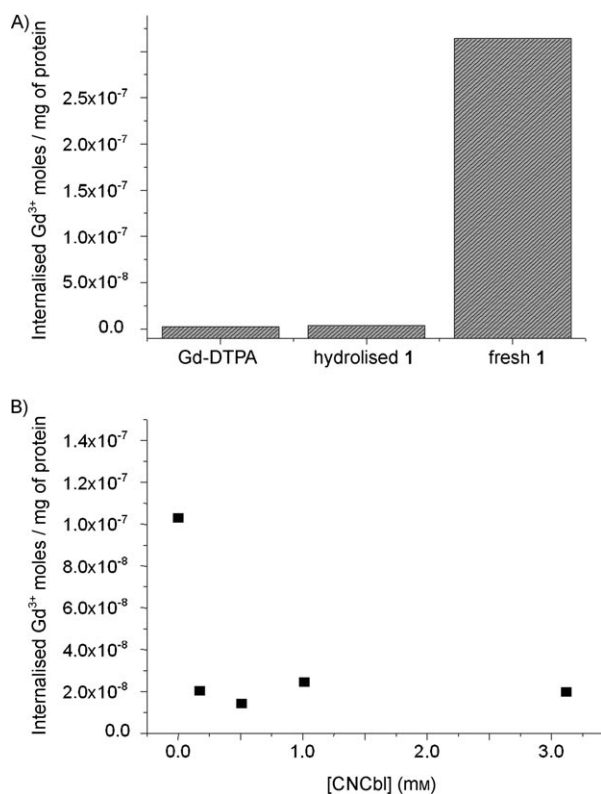


Figure 7. A) Amount of internalised  $Gd^{3+}$  in K562 cells when 1 mM Gd-DTPA, hydrolysed **1** or fresh **1** are added to the incubation medium (37°C, 1 h); B) amount of internalised  $Gd^{3+}$  in K562 cells when 0.46 mM **1** and increasing amounts of CNCbl are added to the incubation medium (37°C, 1 h).

tion medium. At just 0.16 mM of the competitor, the amount of internalised  $Gd^{3+}$  decreases by one order of magnitude.

Finally, viability tests on K562 incubated in the presence of **1** and **2** have been carried out. The Trypan blue test reports the loss of membrane integrity, because the damaged cells appear deeply blue coloured under an optical microscope. Figure 8 shows that when **1** is present in the incubation medium, the cell viability is markedly affected and is reduced to <50% at a concentration of 1 mM of the Gd-containing agent. Conversely, the effect of **2** on cell viability is negligible. As an additional control, the WST-1 test was undertaken. It reports on the mitochondrial functionality and is therefore considered a good complement to the Trypan blue test. As shown in Figure 8B, the obtained results parallel the behaviour observed for the Trypan blue test.

A few years ago it was reported that cells act as “sponges” for free  $Gd^{3+}$  ions if cell labelling is performed with low thermodynamic stability complexes (i.e., Gd-DTPA-BMA).<sup>[30]</sup> A comparison between our CNCbl-targeted system and the non-specific Gd-DTPA-BMA low stabili-

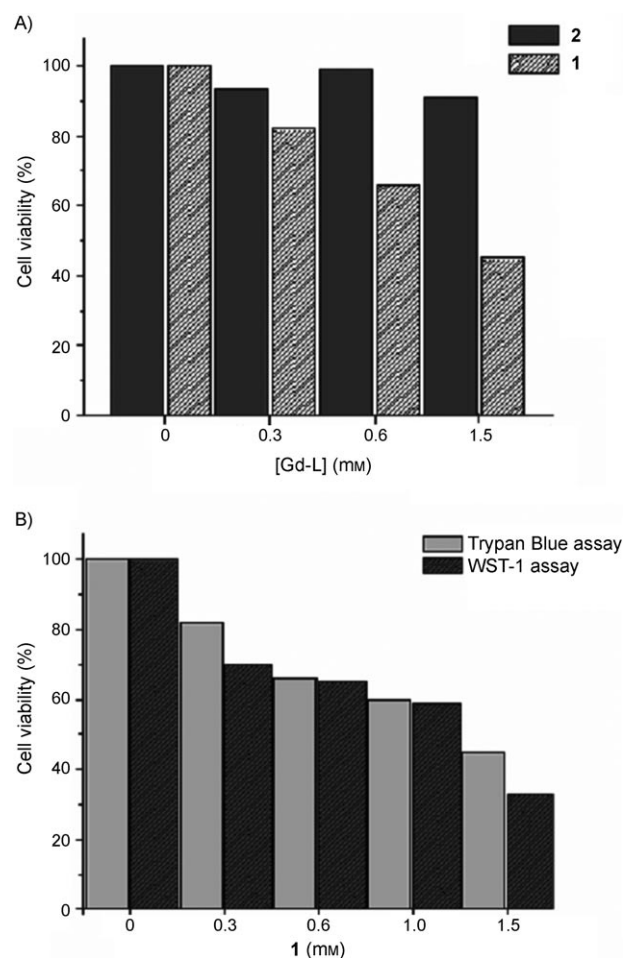


Figure 8. A) Cell viability measured by the Trypan blue assay on K562 cells incubated in the presence of different concentrations of **1** and **2**; B) the results obtained in A for **1** with Trypan blue are compared with the analogous results obtained with the WST-1 assay.

ty ( $\log K = 16.85$ ) complex could be useful: the amount of internalised Gd<sup>3+</sup>, when the same concentration of Gd probe in the incubation media is used, is 3 to 4 times higher for **1** with respect to Gd-DTPA-BMA, even if the thermodynamic stability constant of the former complex is expected to be higher than that of Gd-DTPA-BMA.

One can surmise that in this case the high uptake efficiency shown by K562 cells toward toxic Gd<sup>3+</sup> ions is brought about by the synergy of two effects: on the one hand, the high affinity of **1** for the serum vitamin B<sub>12</sub> transport proteins that bind to the receptors on cells, and on the other hand, the relatively low stability of the Gd complex. Upon binding to receptors, **1** lies on the cellular membrane and likely is establishing hydrogen-bonding interactions between oxygen atoms of the co-ordination cage and surrounding hydrogen donor groups. These hydrogen-bonding interactions remove the negative charge from the donor atoms<sup>[31]</sup> of the ligand, thus decreasing the co-ordination ability and favouring the dissociation of the metal ion. The high toxicity observed for K562 cells treated with **1** appears as a further indication of the massive uptake of Gd<sup>3+</sup> ions.

## Conclusion

We have designed, synthesised and characterised two new bioconjugates of vitamin B<sub>12</sub> resulting from the esterification of the ribose 5'-hydroxyl of CNCbl with the metal-chelating agents DTPA or TTHA. Both Gd<sup>3+</sup>-containing derivatives, **1** and **2**, are able to bind to the plasmatic transport protein, TC, with almost the same high affinity as the parent vitamin B<sub>12</sub>. The major difference between the two bioconjugates is the presence of an open co-ordination shell in the case of DTPA with a possible involvement of the ester functionality in co-ordination. In the case of **2**, the co-ordination number of the Gd<sup>3+</sup> ion is fully saturated by four nitrogen atoms and five carboxylate oxygen atoms, thus avoiding the involvement of the weaker ester functionality in the co-ordination scheme. The involvement of the ester oxygen atom in Gd co-ordination in **1** is responsible for its lower stability towards hydrolysis. Moreover, this causes a significant difference in the ability to release Gd<sup>3+</sup> ions at the binding sites on the cellular membrane. In fact, in the cell-culture experiments with both derivatives, it has been found that free Gd<sup>3+</sup> metal ions are released and avidly taken up specifically by the human immortalised myelogenous leukaemia K562 cells only from bioconjugate **1**. Finally, viability tests on K562 cells incubated in the presence of a relatively low concentration of **1** suggest that the bioconjugate CNCbl-DTPA is able to deliver Gd<sup>3+</sup> ions to cells at a cytotoxic level.

## Experimental Section

**General:** Vitamin B<sub>12</sub>, DTPA dianhydride, TTHA, gadolinium chloride (GdCl<sub>3</sub>·6H<sub>2</sub>O), Dowex 1×2-400 ion-exchange resin and anhydrous pyridine were purchased from Sigma-Aldrich. Acrylamide/*N,N'*-methylene-

bisacrylamide 29:1 solution (40% in H<sub>2</sub>O), ammonium persulfate and buffers of analytical grade were purchased from Fluka. *N,N,N',N'*-Tetramethylethylenediamine (TEMED) was purchased from Amersham Biosciences. Acetone, diethyl ether, acetic anhydride and phenol were provided by Carlo Erba. DMSO was obtained from Fluka and dehydrated on molecular sieves before use.

ESIMS mass spectra were recorded in positive mode by using an API 1 mass spectrometer (Perkin-Elmer) for DTPA-CNCbl and TTHA-CNCbl, and in negative mode using a Bruker ESQUIRE 4000 for **1** and **2**. <sup>1</sup>H and <sup>13</sup>C 1D and edited gHSQC spectra were recorded using a Varian 500 Inova instrument (<sup>1</sup>H at 499 MHz and <sup>13</sup>C at 125.7 MHz). Other NMR spectra (COSY, ROESY) were obtained using a Jeol EX-400 instrument (<sup>1</sup>H at 400 MHz and <sup>13</sup>C at 100.4 MHz).

All manipulations involving CNCbl and its derivatives were carried out in dim light.

**DTPA-CNCbl:** CNCbl (300 mg, 0.22 mmol) and DTPA dianhydride (300 mg, 0.84 mmol) were suspended in anhydrous DMSO (40 mL) and anhydrous pyridine (5 mL). The mixture was stirred for 24 hr at 45 °C. After filtration, water (150 mL) was added and the resulting solution was extracted with aqueous phenol (92%). The first phenol layer was discarded. The combined remaining phenol layers were washed exhaustively with water. One volume of acetone and three volumes of diethyl ether were added to the phenol phase and the resulting organic phase was extracted with water. The combined aqueous layers were washed with diethyl ether to remove residual phenol. The aqueous solution was then concentrated in vacuo and applied to a DOWEX 1×2-400 column (50 g, 3.0×20 cm). The column was first eluted with water to remove residual unreacted CNCbl and then eluted with NaCl (1.0 M). The latter fraction, which contained the desired product, was desalted by phenol extraction (as above). Solid DTPA-CNCbl was obtained by lyophilisation of the final aqueous solution. The lyophilised solid was stored at 4 °C. Yield: 185 mg (49%); <sup>1</sup>H NMR (D<sub>2</sub>O, pD=2.2, DSS; H' and H'' refer to downfield and upfield signals, respectively; for the atom numbering scheme, see Scheme 2): δ = 0.43 (s, 3H; H-C20), 1.02 (m, 2H; H''-C41, H''-C42), 1.21 (s, 3H; H-C46), 1.27 (d, 3H; H-Pr3), 1.41 (s, 3H; H-C54), 1.42 (s, 3H; H-C25), 1.45 (s, 3H; H-C47), 1.77–1.83 (m, 2H; H''-C42, H not assigned), 1.88 (s, 3H; H-C36), 1.88–2.10 (m, 5H; H''-C41, H''-C30, H''-C30, H''-C48, H''-C48), 2.06 (m, 1H; not assigned), 2.20 (d, 1H; H''-C37), 2.28 (s, 6H; H-B10, H-B11), 2.40 (m, 2H; H-C26), 2.48–2.63 (m, 5H; H''-C31, H''-C31, H''-C37, 2H not assigned), 2.56 (s, 3H; H-C35), 2.59 (s, 3H; H-C53), 2.63–2.76 (m, 3H; H''-C49, H''-C49, H not assigned), 2.78 (m, 3H; H''-C18, H''-C18, H not assigned), 3.00 (m, 1H; H''-PR1), 3.35 (m, 3H; H-C13, N-CH<sub>2</sub>CH<sub>2</sub>-N), 3.44 (m, 5H; H-C8, N-CH<sub>2</sub>CH<sub>2</sub>-N, N-CH<sub>2</sub>CH<sub>2</sub>-N), 3.54 (m, 2H; N-CH<sub>2</sub>CH<sub>2</sub>-N), 3.62 (m; H''-PR1), 3.87 (s, 2H; C=OCH<sub>2</sub>-N), 3.90 (s, 2H; C=OCH<sub>2</sub>-N), 3.98 (s, 4H; C=OCH<sub>2</sub>-N), 4.11 (m, 1H; H-C19), 4.15 (m, 2H; C=OCH<sub>2</sub>-N), 4.21 (m, 1H; H-C3), 4.26 (m, 1H; H-R2), 4.32 (m, 1H; H-PR2), 4.36 (m, 1H; H-R5''), 4.70 (m, 1H; H-R5'), 4.88 (m, 1H; H-R3), 6.10 (s, 1H; H-C10), 6.39 (d, 1H; H-R1), 6.52 (s, 1H; H-B4), 7.11 (s, 1H; H-B2), 7.29 ppm (s, 1H; H-B7); H-C55, H-C56 and H-C56 were not assigned; <sup>13</sup>C NMR (D<sub>2</sub>O, pD=2.2, DSS): δ = 18.1 (C53), 18.3 (C35), 18.7 (C54), 19.7 (C25), 21.9 (C36), 21.9 (PR3), 22.1 (C47), 22.2 (C20), 22.3 (B11), 22.8 (B10), 28.8 (C41), 28.9 (C30), 30.7 (C48), 34.2 (C46), 34.4, 34.5 (C42), 35.0, 35.4, 37.6 (C49), 37.8 (C31), 41.9 (C18), 45.7 (C26), 45.8 (C37), 48.1 (PR1), 50.1 (C2), 51.0 (C12), 53.6 (DTPA N-CH<sub>2</sub>-CH<sub>2</sub>), 54.4 (C7), 54.5 (DTPA N-CH<sub>2</sub>-CH<sub>2</sub>, DTPA N-CH<sub>2</sub>-CH<sub>2</sub>), 54.6 (DTPA N-CH<sub>2</sub>-CH<sub>2</sub>), 56.7 (C13), 57.6 (DTPA CH<sub>2</sub>C=O), 57.8 (DTPA CH<sub>2</sub>C=O), 58.6 (C8), 59.0 (C3), 59.0 (DTPA CH<sub>2</sub>C=O), 59.2 (DTPA CH<sub>2</sub>C=O), 62.1 (C17), 66.4 (R5), 71.6 (R2), 75.9 (PR2), 75.9 (R3), 77.8 (C19), 81.9 (R4), 88.0 (C1), 90.0 (R1), 97.8 (C10), 107.0 (C15), 110.4 (C5), 114.3 (B7), 119.4 (B4), 132.8 (B8), 136.0 (B5), 138.1 (B6), 139.5 (B9), 144.6 (B2), 168.2 (C6), 168.9 (C14), 172.6 (DTPA COOH), 174.0 (DTPA COOH), 175.0 (DTPA COOH), 175.2 (DTPA COOH), 176.4, 177.5, 178.0, 178.6, 178.7, 179.7, 179.9, 180.5, 180.7, 181.8, 182.9 ppm; UV/Vis (H<sub>2</sub>O): λ (ε) = 361 nm (2.7×10<sup>4</sup> mol<sup>-1</sup> dm<sup>3</sup> cm<sup>-1</sup>); ESIMS (120 V, H<sub>2</sub>O): *m/z* calcd (%) for C<sub>77</sub>H<sub>109</sub>CoN<sub>17</sub>O<sub>23</sub>P: 1730.7; found: 899.4 (100) [M-H<sup>+</sup>+3Na<sup>+</sup>], 1731.3 (7) [M+H<sup>+</sup>].

**TTHA-CNCbl:** The compound was synthesised by following the same method as that described for DTPA-CNCbl, starting from CNCbl and

TTHA dianhydride. Yield: 120 mg (30%);  $^1\text{H NMR}$  ( $\text{D}_2\text{O}$ ,  $\text{pD}=2.2$ , DSS; H' and H'' refer to downfield and upfield signal, respectively):  $\delta=0.47$  (s, 3H; H-C20), 1.03 (m, 2H; H''-C41, H''-C42), 1.20 (s, 3H; H-C46), 1.26 (d, 3H; H-Pr3), 1.40 (s, 3H; H-C54), 1.42 (s, 3H; H-C25), 1.45 (s, 3H; H-C47), 1.77–1.83 (m, 2H; H'-C42), H not assigned), 1.88 (s, 3H; H-C36), 1.88–2.10 (m, 5H; H'-C41, H'-C30, H''-C30, H'-C48, H''-C48), 2.08 (m, 1H; H not assigned), 2.20 (d, 1H; H''-C37), 2.26 (s, 6H; H-B10, H-B11), 2.43 (m, 2H; H-C26), 2.48–2.63 (m, 4H; H'-C31, H''-C31, H'-C37, H not assigned), 2.55 (s, 3H; H-C35), 2.59 (s, 3H; H-C53), 2.63–2.73 (m, 4H; H'-C49, H''-C49, 2H not assigned), 2.76 (m, 3H; H'-C18, H''-C18, H not assigned), 3.00 (m, 1H; H''-PR1), 3.26–3.36 (m, 7H; H-C13, N- $\text{CH}_2\text{CH}_2\text{-N}$ ), 3.43 (m, 3H; H-C8, N- $\text{CH}_2\text{CH}_2\text{-N}$ ), 3.49 (m, 4H; N- $\text{CH}_2\text{CH}_2\text{-N}$ ), 3.62 (m; H'-PR1), 3.75 (s, 2H; C= $\text{OCH}_2\text{-N}$ ), 3.80 (s, 2H; C= $\text{OCH}_2\text{-N}$ ), 3.99 (s, 8H; C= $\text{OCH}_2\text{-N}$ ), 4.10 (m, 1H; H-C19), 4.20 (m, 1H; H-C3), 4.28 (m, 1H; H-R4), 4.32 (m, 3H; H-PR2, H-R2, H-R5''), 4.68 (m, 1H; H-R5'), 4.88 (m, 1H; H-R3), 6.08 (s, 1H; H-C10), 6.37 (d, 1H; H-R1), 6.51 (s, 1H; H-B4), 7.11 (s, 1H; H-B2), 7.29 ppm (s, 1H; H-B7); H-C55, H-C56 and H-C56 were not assigned;  $^{13}\text{C NMR}$  ( $\text{D}_2\text{O}$ ,  $\text{pD}=2.2$ , DSS):  $\delta=18.1$  (C53), 18.3 (C35), 18.8 (C54), 19.7 (C25), 21.9 (C36), 22.0 (PR3), 22.1 (C47), 22.2 (C20), 22.3 (B11), 22.8 (B10), 28.8 (C41), 28.9 (C30), 30.7 (C48), 34.2 (C46), 34.3, 34.5 (C42), 35.0, 35.2, 37.6 (C49), 37.8 (C31), 41.9 (C18), 45.7 (C26), 45.8 (C37), 48.2 (PR1), 50.1 (C2), 51.0 (C12), 52.7 (TTHA N- $\text{CH}_2\text{-CH}_2$ ), 53.3 (TTHA N- $\text{CH}_2\text{-CH}_2$ ), 53.5 (TTHA N- $\text{CH}_2\text{-CH}_2$ ), 54.4 (C7), 54.8 (TTHA N- $\text{CH}_2\text{-CH}_2$ ), 55.3 (TTHA N- $\text{CH}_2\text{-CH}_2$ ), 56.0 (TTHA N- $\text{CH}_2\text{-CH}_2$ ), 56.7 (C13), 57.4 (TTHA  $\text{CH}_2\text{C=O}$ ), 57.9 (TTHA  $\text{CH}_2\text{C=O}$ ), 58.2 (DTPA  $\text{CH}_2\text{C=O}$ ), 58.6 (C8), 58.7 (TTHA  $\text{CH}_2\text{C=O}$ ), 59.1 (C3), 59.3 (TTHA  $\text{CH}_2\text{C=O}$ , TTHA  $\text{CH}_2\text{C=O}$ ), 62.1 (C17), 66.4 (R5), 71.6 (R2), 75.9 (PR2), 76.2 (R3), 77.8 (C19), 82.0 (R4), 88.0 (C1), 90.0 (R1), 97.8 (C10), 107.0 (C15), 110.4 (C5), 114.3 (B7), 119.3 (B4), 132.8 (B8), 135.9 (B5), 138.0 (B6), 139.5 (B9), 144.6 (B2), 168.1 (C6), 169.0 (C14), 173.6 (TTHA COOH), 173.7 (TTHA COOH, TTHA COOH), 174.2 (TTHA COOH), 176.0 (TTHA COOH), 176.4 (C9), 176.8 (TTHA COOH), 177.5 (C57), 177.9 (C38), 178.5 (C61), 178.6 (C27), 179.7 ppm (C11); UV/Vis ( $\text{H}_2\text{O}$ ):  $\lambda$  ( $\epsilon$ )=361 nm ( $2.7 \times 10^4 \text{ mol}^{-1} \text{ dm}^3 \text{ cm}^{-1}$ ); ESIMS (120 V,  $\text{H}_2\text{O}$ ):  $m/z$  calcd (%) for  $\text{C}_{69}\text{H}_{116}\text{CoN}_{18}\text{O}_{25}\text{P}$ : 1831.8; found: 916.9 (100) [ $M+2\text{H}^+$ ], 1831.9 (7) [ $M+\text{H}^+$ ].

**Gd–DTPA–CNCbl (in situ) (1):** Complex **1** was prepared in situ by treating aqueous solutions of DTPA–CNCbl with  $\text{GdCl}_3$  (0.9 equiv) dissolved in water at the desired pH and concentration. The solutions were prepared immediately prior to use or kept in a freezer for long-time storage, to avoid the hydrolysis of the ester bond. HRMS (ESI):  $m/z$  calcd (%) for  $\text{C}_{77}\text{H}_{105}\text{CoN}_{17}\text{O}_{23}\text{PGd}$ : 1883.9; found: 1883.7 (100) [ $M^+$ ].

**Gd–TTHA–CNCbl (in situ) (2):** Complex **2** was prepared following the same procedure described for **1**, starting from TTHA–CNCbl. HRMS (ESI):  $m/z$  calcd (%) for  $\text{C}_{51}\text{H}_{111}\text{CoN}_{18}\text{O}_{25}\text{PGd}$ : 1984.01; found: 1984.7 (100) [ $M^+$ ].

**Characterisation by PAGE:** Polyacrylamide gels (16%) were prepared by mixing filtered deionised water (2.45 mL), acrylamide/bis(acrylamide) solution (29:1; 2 mL, 40%), buffer solution (0.5 mL; 0.5 M HEPES, 0.5 M boric acid, pH 7.2 adjusted with NaOH), ammonium persulfate (50  $\mu\text{L}$ , 10%) and TEMED (5  $\mu\text{L}$ ). The PAGE analysis was run on a Hoefer SE250 vertical gel electrophoresis unit from Amersham Biosciences using as running buffer a 10-fold dilution of the buffer solution used for gel preparation.

**X-ray crystallography:** Recrystallisation of **1** was carried out using the hanging-drop vapour-diffusion technique at 293 K.  $\text{Gd}^{3+}$  from  $\text{GdCl}_3$  was added to **1** in an excess of 1.3:1 to ensure full occupancy of the  $\text{Gd}^{3+}$  site in the bioconjugate. Complex **1** (100 mM, 1  $\mu\text{L}$ ) was mixed with reservoir solution (40% v/v PEG 400 and 3.4 M LiCl, 1  $\mu\text{L}$ ). Small crystals with the shape of a biconvex lens were obtained in a few hours and some continued to grow for about a week to a final size of approximately 0.25 mm  $\times$  0.1 mm  $\times$  0.05 mm. X-ray diffraction data were collected using a Bruker–Nonius FR591 rotating Cu anode equipped with a KappaCCD diffractometer and an Oxford cryosystem for data collection at a temperature of 100 K. The structure was solved using the single-wavelength anomalous dispersion method. Sites of heavy atoms (Gd, Co, P) were found with SHELXD and phases to 1.44 Å resolution were calculated with

SHELXE from the SHELX-97 programme package.<sup>[32]</sup> Restrained refinement of the structure was performed with SHELXL using anisotropic B-factors only for the heavy atoms and ordered solvent ions ( $\text{Cl}^-$ ,  $\text{Na}^+$ ). Hydrogen atoms and 42 solvent water molecules were added during structure refinement. The crystallographic statistics of **1** are as follows: resolution range 40–1.44 Å; space group C222<sub>1</sub>;  $a=17.614$ ,  $b=38.124$ ,  $c=42.529$  Å; 3026 unique reflections;  $R_{\text{merge}}=9.6\%$  (1.55–1.44 Å: 32.5%);  $I/\sigma=8.4$  (1.55–1.44 Å: 3.1); completeness 96.6% (1.55–1.44 Å: 83.2%);  $R$  factor (all  $F_{\text{obs}}$ ) 13.6%;  $R$  factor ( $F_{\text{obs}} > 4\sigma$ ) 12.7%; Gd–DTPA–CNCbl (121 atoms including  $\text{H}_2\text{O}$  ligands):  $B=12.1$  Å<sup>2</sup>; bulk solvent (46 atoms including 2  $\text{Na}^+$ , 2  $\text{Cl}^-$ ):  $B=28.1$  Å<sup>2</sup>.

CCDC-697308 contains the supplementary crystallographic data for this paper. These data can be obtained free of charge from The Cambridge Crystallographic Data Centre via [www.ccdc.cam.ac.uk/data\\_request/cif](http://www.ccdc.cam.ac.uk/data_request/cif).

#### Kinetics of binding to and dissociation from the transport proteins TC:

The binding and dissociation experiments were performed as described earlier.<sup>[27,29]</sup> In short, a mixture of **1** (0–2  $\mu\text{M}$ ) and a fluorescent Cbl analogue CBC (0.5  $\mu\text{M}$ ) was injected into the binding protein IF or TC (0.5  $\mu\text{M}$ ). Afterwards, the increase in fluorescence was measured due to higher quantum yield of the complexes IF–CBC and TC–CBC when compared with the free fluorescent probe CBC (excitation wavelength 525 nm, bandpass 7 nm, 550 nm cut-off filter on the emission side). The presence of the non-fluorescent ligand **1** (or **2**) in the reaction medium caused a suppression of the registered response because of competition between **1** (or **2**) and CBC for the binding site. The binding reaction was conducted in an Na-phosphate buffer (0.2 M, pH 7.5, 20 °C). Measurement of the dissociation rate constant was based on a chase experiment, where the pre-incubated protein–ligand complex IF–**1** (or IF–**2**) or TC–**1** (or TC–**2**) (0.5  $\mu\text{M}$ ) was mixed with an excess of the fluorescent ligand CBC (1  $\mu\text{M}$ ). Then the increase in fluorescence was measured over time due to dissociation of **1** (or **2**) and formation of IF–CBC or TC–CBC. Reaction conditions were as mentioned above.

**In vitro cellular uptake:** K562 cells were grown in RPMI 1640 medium containing foetal bovine serum (10%). Cells were seeded to a density of  $1 \times 10^6$  cells  $\text{mL}^{-1}$  into 60 mm culture dishes. The cells were incubated at 37 °C for 1 h in culture media containing increasing amounts (from 0.2 to 1.2 mM) of **1** and **2**. After this treatment, the cells were washed three times with ice-cold phosphate-buffered saline (PBS) (5 mL).

**Determination of  $\text{Gd}^{3+}$  content in cells:** At the end of the uptake experiment, labelled cells were collected in PBS (200  $\mu\text{L}$ ) and were sonicated for 10 s for a complete lysis, added to the same volume of HCl (37%) and left at 120 °C overnight. Upon this treatment all  $\text{Gd}^{3+}$  was solubilised as free aquo-ion. By measuring the relaxation rates of these solutions at 20 MHz and 25 °C using a Stellar Spinmaster spectrometer (Stellar, Mede, Pavia, Italy), it is possible to determine its concentration.

The obtained  $R_{\text{obs}}$  data are related to the concentration of the paramagnetic species according to Equation (1):

$$R_{\text{obs}} = R_{1\text{W}} + [\text{Gd}^{3+}] \cdot r_{1\text{pGd}^{3+}} \quad (1)$$

in which  $R_{1\text{W}}$  is the relaxation rate of pure water (0.38  $\text{s}^{-1}$ ) and  $r_{1\text{pGd}^{3+}}$  the millimolar relaxivity of the  $\text{Gd}^{3+}$  ion (13.5  $\text{mm}^{-1} \text{s}^{-1}$  in a 6 M HCl solution). Moles of  $\text{Gd}^{3+}$  obtained in this way were normalised to the weight (mg) of cellular proteins. The protein concentration of each sample was determined from cell lysates by the Bradford method using bovine serum albumin as standard. One milligram of protein corresponds to about  $4.5 \times 10^6$  cells.

**Cell viability tests:** The Trypan blue exclusion test was used to assess cell viability. An aliquot (10  $\mu\text{L}$ ) of each cell suspension, both control and treated cells, was mixed with an equal amount of Trypan blue solution (0.4%) in PBS. An aliquot (10  $\mu\text{L}$ ) of the solution was introduced in a counting chamber (hemocytometer). Viable cells were found in shape and bright, whereas damaged cells appeared deep blue due to the incorporation of the Trypan dye. Viability was expressed as a percentage (ratio between viable cells and total cells  $\times 100$ ). Cell viability was also assessed by the WST-1 (Roche) test. Briefly, K562 cells seeded in 3.5 cm Petri dishes were used to carry out the uptake experiments with **1**. Subsequently, the WST-1-containing solution was added to each dish in 1:10

ratio (v/v). WST-1 is a tetrazolium salt that was reduced to formazan by mitochondrial dehydrogenases. The cells were incubated for 1 h at 37°C under an atmosphere of pCO<sub>2</sub> (5%). After incubation, the solution was diluted to a ratio of 1:10 in PBS and the absorbance at 440 nm was measured. A solution of WST in the culture medium without cells served as control. The measured absorbance reflected the tetrazolium to formazan transformation and it probed the cell viability in terms of functionality of the mitochondrial machinery. For optimal activity, the absorbance displays values of approximately 0.6–0.7.

**Hydrolysis of 1 and 2:** The hydrolysis equilibrium of complexes **1** and **2** has been followed by measuring the time course of the water proton relaxation rates of 1 mM solutions of each complex in phosphate-buffered saline at pH 7.2 and 298 K.

The longitudinal water proton relaxation rate was measured by using a Stelar Spinmaster spectrometer operating at 20 MHz, by means of the standard inversion–recovery technique. The temperature was controlled with a Stelar VTC-91 airflow heater equipped with a copper constantan thermocouple (uncertainty 0.1°C).

Hydrolysis of the Eu analogue of **1** (Eu-**1**) was investigated by collecting <sup>31</sup>P NMR spectra of a solution (7 mM) of the Eu-**1** in HEPES buffer at pH 7.2 and 298 K over time. The reaction was followed by monitoring the decrease of intensity of the Eu-**1** <sup>31</sup>P resonance at  $\delta = 0.76$  ppm (from H<sub>3</sub>PO<sub>4</sub> 85%) and the concomitant increase of intensity of the resonance of CNCbl at  $\delta = 0.025$  ppm.

NMR spectra have been registered by using a Bruker Avance 600 spectrometer and by using a capillary tube containing D<sub>2</sub>O for lock control and H<sub>3</sub>PO<sub>4</sub> as chemical shift reference.

Hydrolysis of **1** was also studied by means of a PAGE experiment. Preincubated samples of **1** in phosphate-buffered saline at pH 7.28 at 37°C were quenched at regular intervals by addition of HCl and stored at –20°C. The samples were run on PAGE as described above.

## Acknowledgements

Economic and scientific support from MIUR (FIRB RBNE03PX83, FIRB RBIP06293N and PRIN 2007W7M4NF projects), Friuli-Venezia-Giulia region (DPRReg. 120/2007/Pres.), EC-FP6-projects (LSHB-CT-2005-512146), EMIL (LSHC-CT-2004-503569), MEDITRANS (Targeted Delivery of Nanomedicine: NMP4-CT-2006-026668) and EU-COST D38 Action is gratefully acknowledged.

- [1] R. Banerjee, S. W. Ragsdale, *Annu. Rev. Biochem.* **2003**, *72*, 209–247.
- [2] R. Waibel, H. Treichler, N. G. Schaefer, D. R. van Staveren, S. Mundwiler, S. Kunze, M. Küenzi, R. Alberto, J. Nüesch, A. Knuth, H. Moch, R. Schibli, P. A. Schubiger, *Cancer Res.* **2008**, *68*, 2904–2911.
- [3] R. Banerjee, *ACS Chem. Biol.* **2006**, *1*, 149–159.
- [4] M. Wolters, A. Strohle, A. Hahn, *Prev. Med.* **2004**, *39*, 1256–1266.
- [5] H. P. C. Hogenkamp, D. A. Collins, C. B. Grissom, F. G. West in *Chemistry and Biochemistry of Vitamin B<sub>12</sub>* (Ed.: R. Banerjee), Wiley, New York, **1999**, pp. 385–410.
- [6] G. Russell-Jones, K. McTavish, J. McEwan, J. Rice, D. Nowotnik, *J. Inorg. Biochem.* **2004**, *98*, 1625–1633.
- [7] G. R. McLean, P. M. Pathare, D. S. Wilbur, A. C. Morgan, S. V. Woodhouse, J. W. Schrader, H. J. Ziltener, *Cancer Res.* **1997**, *57*, 4015–4022.
- [8] D. A. Collins, H. P. C. Hogenkamp, *J. Nucl. Med.* **1997**, *38*, 717–723.
- [9] D. A. Collins, H. P. C. Hogenkamp, M. K. O'Connor, S. Naylor, L. M. Benson, T. J. Hardyman, L. M. Thorson, *Mayo Clin. Proc.* **2000**, *75*, 568–580.
- [10] C. C. Smeltzer, M. J. Cannon, P. R. Pinson, J. D. Munger, F. G. West, C. B. Grissom, *Org. Lett.* **2001**, *3*, 799–801.
- [11] J. M. McGreevy, M. J. Cannon, C. B. Grissom, *J. Surg. Res.* **2003**, *111*, 38–44.
- [12] J. D. Bagnato, A. L. Eilers, R. A. Horton, C. B. Grissom, *J. Org. Chem.* **2004**, *69*, 8987–8996.
- [13] T. Amagasaki, R. Green, D. W. Jacobsen, *Blood* **1990**, *76*, 1380–1386.
- [14] D. A. Collins, H. P. C. Hogenkamp, M. K. O'Connor, S. Naylor, L. M. Benson, T. J. Hardyman, L. M. Thorson, *Mayo Clin. Proc.* **2000**, *75*, 568–580.
- [15] D. A. Collins, H. P. C. Hogenkamp, M. W. Gebhard, *Mayo Clin. Proc.* **1999**, *74*, 687–691.
- [16] J. Wuerges, G. Garau, S. Geremia, S. N. Fedosov, T. E. Petersen, L. Randaccio, *Proc Natl Acad Sci USA* **2006**, *103*, 4386–4391.
- [17] J. Wuerges, S. Geremia, L. Randaccio, *Biochem. J.* **2007**, *403*, 431–440.
- [18] J. Reubi, J. C. Schaer, B. Waser, S. Wenger, A. Heppeler, J. S. Schmitt, H. R. Maecke, *Eur. J. Nucl. Med. Mol. Imaging* **2000**, *27*, 273–282.
- [19] J. Wuerges, S. Geremia, S. N. Fedosov, L. Randaccio, *IUBMB Life* **2007**, *59*, 722–729.
- [20] T. Toraya, K. Ohashi, H. Ueno, S. Fukui, *Bioinorg. Chem.* **1975**, *4*, 245–255.
- [21] A. M. Calafat, L. G. Marzilli, *J. Am. Chem. Soc.* **1993**, *115*, 9182–9190.
- [22] R. H. Horton, J. D. Bagnato, C. B. Grissom, *J. Org. Chem.* **2003**, *68*, 7108–7111.
- [23] R. B. Hannak, S. Gschösser, K. Wurst, B. Kräutler, *Monatsh. Chem.* **2007**, *138*, 899–907.
- [24] P. Caravan, *Chem. Soc. Rev.* **2006**, *35*, 512–523.
- [25] A. Bianchi, L. Calabi, F. Corana, S. Fontana, P. Losi, A. Maiocchi, L. Paleari, B. Valtancoli, *Coord. Chem. Rev.* **2000**, *204*, 309–393.
- [26] A. D. Sherry, W. P. Cacheris, K.-T. Kuan, *Magn. Reson. Med.* **1988**, *8*, 180–190.
- [27] S. N. Fedosov, C. B. Grissom, N. U. Fedosova, S. K. Moestrup, E. Nexø, T. E. Petersen, *FEBS J.* **2006**, *273*, 4742–4753.
- [28] P. Mendes, *Trends Biochem. Sci.* **1997**, *22*, 361–363.
- [29] S. N. Fedosov, N. U. Fedosova, B. Kräutler, E. Nexø, T. E. Petersen, *Biochemistry* **2007**, *46*, 6446–6458.
- [30] C. Cabella, S. Geninatti Crich, D. Corpillo, A. Barge, C. Girelli, E. Bruno, V. Lorusso, F. Uggeri, S. Aime, *Contrast Media Mol. Imaging* **2006**, *1*, 23–29.
- [31] Z. Baranyai, E. Gianolio, K. Ramalingam, R. Swenson, R. Ranganathan, E. Brucher, S. Aime, *Contrast Media Mol. Imaging* **2007**, *2*, 94–102.
- [32] G. M. Sheldrick, T. R. Schneider, *Methods Enzymol.* **1997**, *277*, 319–343.

Received: December 19, 2008

Revised: April 20, 2009

Published online: June 27, 2009